Stresses in sprayed concrete tunnel linings at Heathrow Terminal 4

B. D. JONES [a,*], C. GRAND [b] and C. R. I. CLAYTON [c]

[a] Inbye Engineering Limited, Coventry CV1 2NP, UK

[b] Zengaffinen AG, Alustrasse 2, CH-3940 Steg, Switzerland

[c] School of Engineering, University of Southampton, Southampton SO17 1BJ, UK

* *Corresponding Author:* bjones@inbye.co.uk

1 Abstract

A wide variety of instrumentation was deployed during construction of the sprayed concrete lined tunnels at Heathrow Express Terminal 4 Station in the mid-1990s, some of which continues to function and be accessible for the taking of readings today. This paper presents a nearly 20-year history of stress in the primary lining of the Concourse Tunnel measured using radial and tangential pressure cells on and in the sprayed concrete. Data from tangential pressure cells require careful interpretation and the new and complete methodology for achieving reliable results described in Jones & Clayton (2021) was used to provide the stress history from construction into the long-term. This is a unique case study, in terms of both the detail of the measurements and interpretation and the time period over which measurements have been taken. The results show that pressure cells are very sensitive and respond to changes in stress due to nearby construction activities, and that after construction has ceased, stresses stabilise at a value well below full overburden pressure (the vertical total stress at tunnel axis level).

2 Introduction

The main tunnels at Heathrow Express Terminal 4 station were constructed between May 1994 and November 1996. To confirm the adequacy of design, particularly of the sprayed concrete primary

lining, a considerable array of instrumentation was installed and monitored during construction. In previous papers the movements ahead of the advancing Concourse Tunnel (van der Berg et al., 2003), and the in-tunnel displacements and surface settlements (Clayton et al., 2006) were presented. An earlier paper by Clayton et al. (2002) studied the performance of pressure cells in sprayed concrete linings, focussing mainly on laboratory tests and numerical modelling to improve understanding of cell action factor, temperature sensitivity and installation effects, but did not present a complete set of field data. Jones & Clayton (2021) built on and refined the interpretation of Clayton et al. (2002), allowing a complete interpretation of stresses in a sprayed concrete primary lining in this paper, where the whole data set, including more recent data, are included, making this a unique, nearly 20-year case study of sprayed concrete lining stress.

In tunnels with segmental linings the maximum load has always been found to occur in the long-term. Skempton (1943) found the maximum load to be approximately equal to that corresponding to the hydrostatic full overburden pressure (that is, the initial in situ total stress with $K_0 = 1.0$). Ward & Thomas (1965) found that one of the tunnels they studied reached full overburden pressure, while the second one did not but was continuing to increase when measurements ceased. They therefore concluded that hydrostatic full overburden pressure would eventually act on the lining in the long-term. Since then, measurements by Muir Wood (1969), Barratt et al. (1994) and Bowers & Redgers (1996), amongst others, have all shown that load can stabilise at a value well below that corresponding to full overburden pressure.

The distribution of stress in a sprayed concrete lined tunnel and how this stress evolves over time has not been well studied and has received nowhere near as much attention as the deformations of the ground and lining (van der Berg et al., 1998b). The main reason for this is the difficulty in obtaining reliable measurements of stress throughout the life of the sprayed concrete from construction into the long-term, and the commitment of the client and other parties required to continue monitoring beyond the construction period. This paper seeks to address this gap by

providing high quality data that can enhance understanding of how ground loads come onto sprayed concrete linings during construction and in the long term, which can be used for the calibration of empirical and numerical predictions.

3 The construction of the Concourse Tunnel

The layout, geology, construction sequence and construction details of the concourse and platform tunnels are described in van der Berg et al. (2003) and Clayton et al. (2006), but important details will be replicated here. The layout of the Heathrow Express Terminal 4 station is shown in Figure 1. It consists of two platform tunnels with a central Concourse Tunnel at the North-eastern end. These tunnels are connected by a series of cross passages and connected to the North and South Ventilation Tunnels at each end, which were constructed after the Concourse Tunnel. The Downline Ventilation Tunnel, which connects the North Ventilation Tunnel to the Downline Platform Tunnel, underpassed the Concourse Tunnel while the Concourse Tunnel was itself being constructed. These events will be highlighted when the stress results are presented.

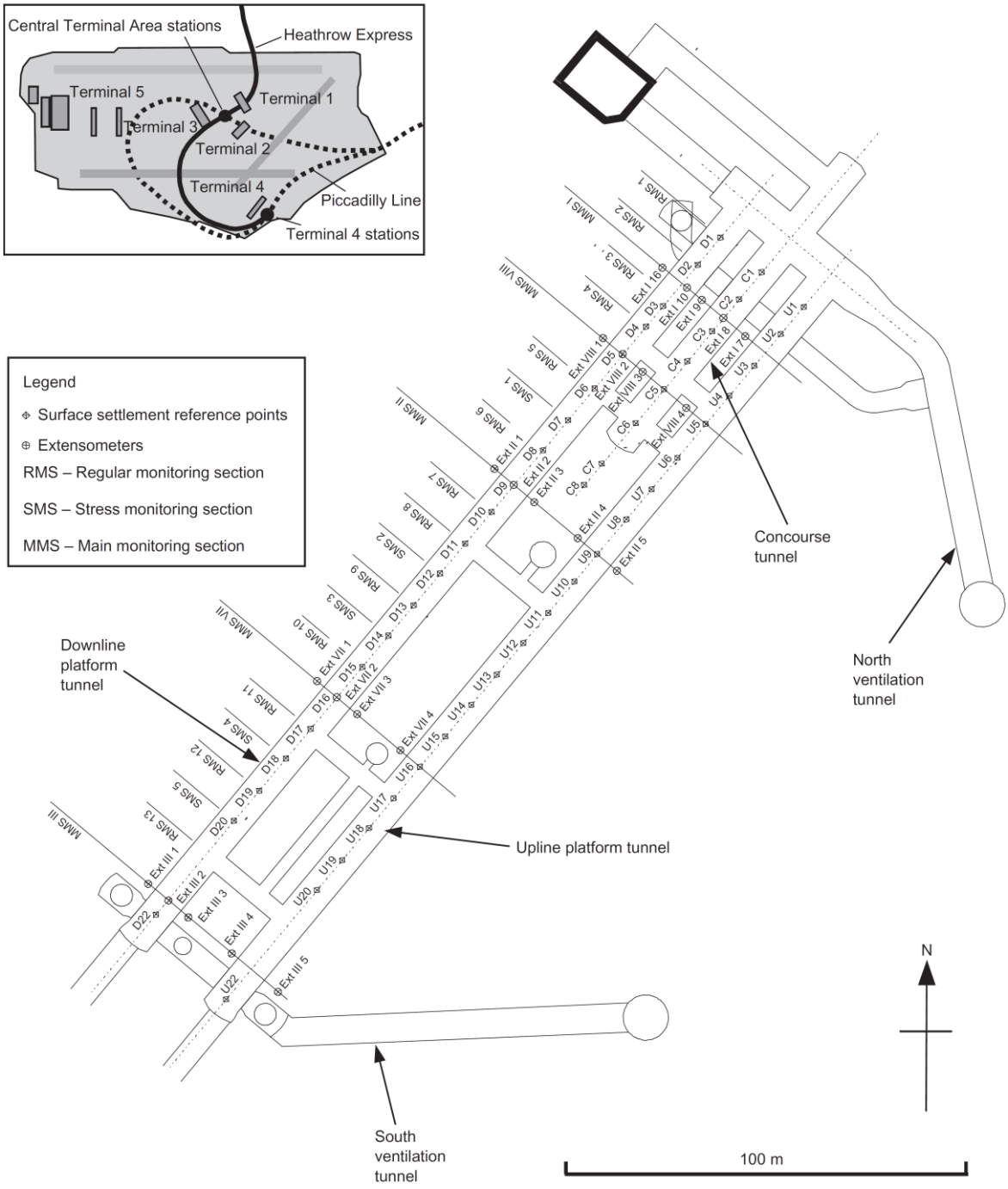

Figure 1: Plan of tunnels at Heathrow Express Terminal 4 station, showing location of Concourse Tunnel and layout of monitoring points and instruments (from van der Berg et al., 2003).

The Platform Tunnels are over 220 m long with a cross-sectional area of 62 m^2, and the Concourse Tunnel is 64 m long with a cross-sectional area of 49 m^2. A cross-section of the Concourse and Platform Tunnels is shown in Figure 2, which also shows the surface level and geological strata. The Concourse Tunnel axis is at a depth of 17.2 m below ground level and the tunnel is entirely within the London Clay. Detailed identification of stratigraphy by Hight et al. (2007) for the Heathrow

Terminal 5 project suggests that the Concourse Tunnel is approximately in the middle of the 25 m thick B2 unit of the London Clay according to the lithological division by King (1981). Piezometers across the site and at different depths indicated a piezometric level in the Terrace Gravels at approximately ground level with a hydrostatic distribution from there down to the basal beds of the London Clay, well below the tunnel horizon (van der Berg et al., 2003). The centreline spacing between the Concourse Tunnel and the Platform Tunnels is 13.5 m.

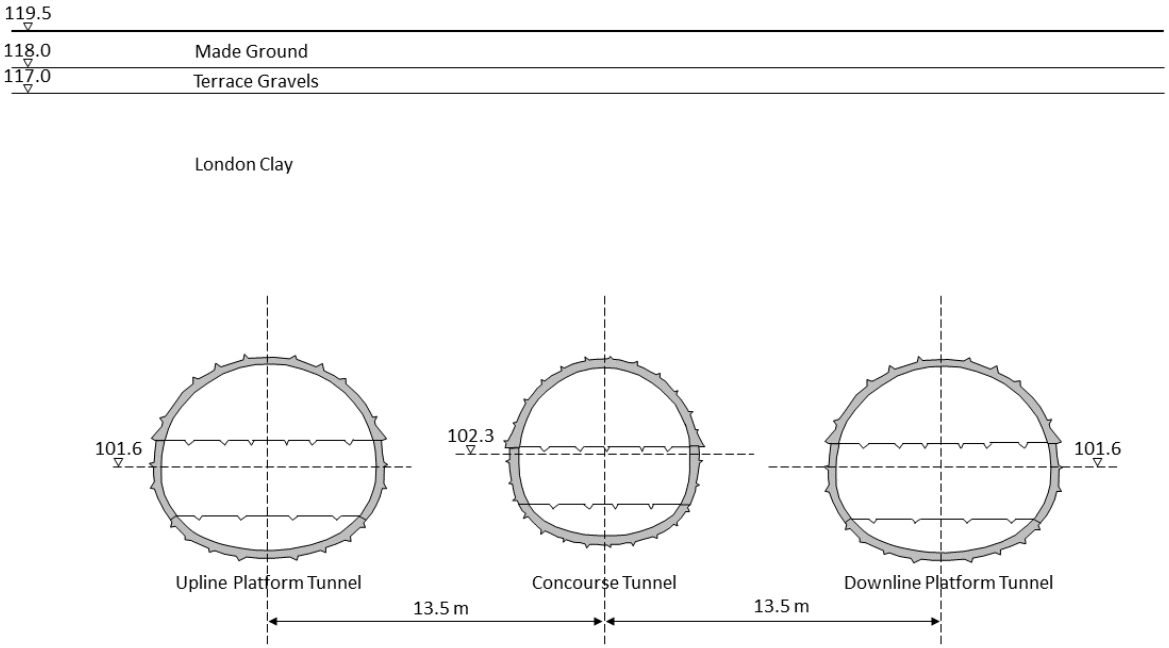

Figure 2: Cross-section of Concourse and Platform Tunnels

Tunnelling works started at Terminal 4 on 10th May 1994 but were suspended by the end of October 1994 following the collapse of the sprayed concrete lined Concourse and Platform Tunnels at Heathrow's Central Terminal Area (HSE, 1996), approximately 1.5 km North of the Terminal 4 station. At the time of the collapse approximately 25 m of the Downline Platform Tunnel and 65 m of the Upline Platform Tunnel at Terminal 4 had been constructed, both commencing from the North Ventilation Tunnel.

Tunnelling works at Terminal 4 resumed with Downline Platform Tunnel construction on 15th September 1995, followed by the Upline Platform Tunnel on 2nd December 1995. Construction of the Concourse Tunnel commenced in September 1996 after completion of the adjacent sections of the

permanent secondary lining in the Upline and Downline Platform Tunnels. The Concourse Tunnel headwall was completed on 7th November 1996.

The construction sequence for the Concourse Tunnel used a top heading, bench, top heading, bench, double-invert sequence. The invert was closed five rounds from the face. The construction sequence is schematically illustrated in Figure 3. A detailed description is provided in the Supplementary Information. The advance length varied from 0.8 m to 1.2 m depending on ground conditions and design requirements, including the proximity of sensitive structures. The primary support for the Concourse Tunnel consisted of 350 mm of sprayed concrete (shotcrete), reinforced with two layers of welded wire mesh and full-section lattice girders.

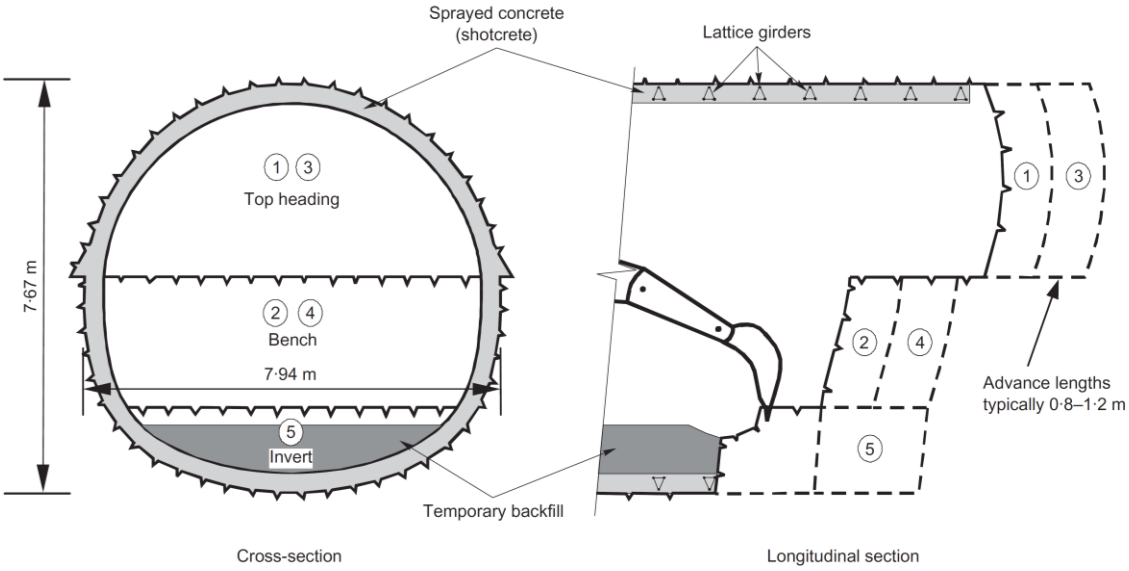

Figure 3: Concourse Tunnel construction sequence (from van der Berg et al., 2003)

This paper will focus on the pressure cells installed in Main Monitoring Section I (MMS I) and Main Monitoring Section VIII (MMS VIII) of the Concourse Tunnel. The locations of these sections are shown in Figure 4 and in the location plan (Figure 1). Both monitoring sections were installed in the second top heading of the repeating 5-stage sequence shown in Figure 3. This is also illustrated in the 'Additional Information' file where the relative positions of the partial excavation faces are shown at the time of each pressure cell reading.

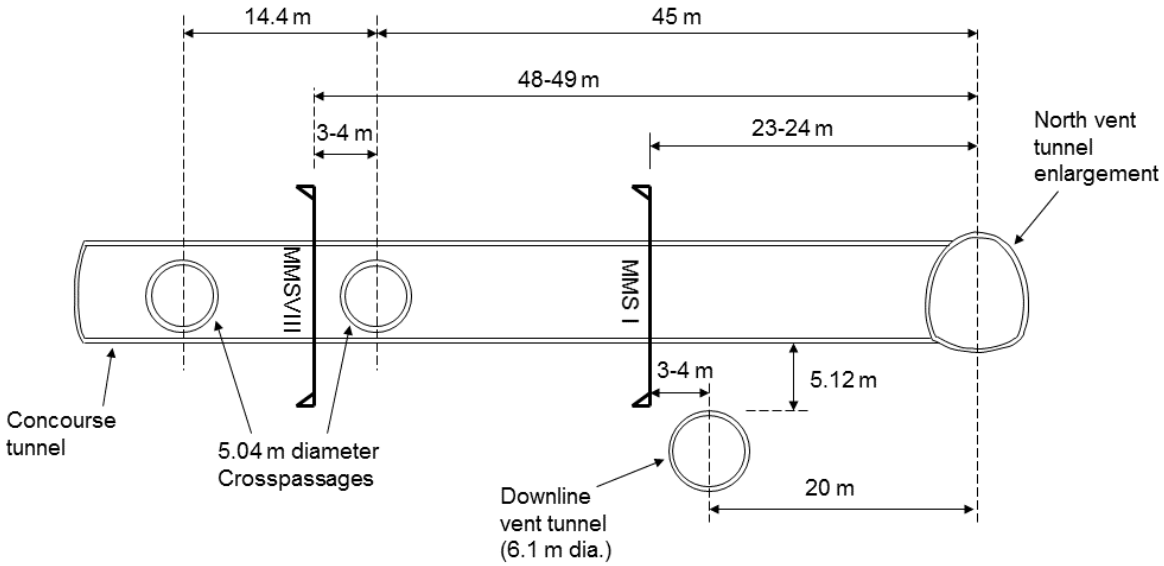

Figure 4: Long section of the Concourse Tunnel showing locations of MMS I and MMS VIII

At each section, 12 tangential pressure cells and 12 radial pressure cells were installed. The locations are shown in Figure 5. In MMS I there were no tangential pressure cells installed at positions 10 and 11, but positions 4 and 5 were equipped with two tangential pressure cells, one near the extrados and one near the intrados. In MMS VIII again no tangential pressure cells were installed at positions 10 and 11, but two were installed at positions 6 and 7 near the extrados and intrados. Where two tangential cells were installed at the same position, the 'OUT' one was centred 110 mm from the extrados and the 'IN' one was centred 230 mm from the extrados and 120 mm from the intrados.

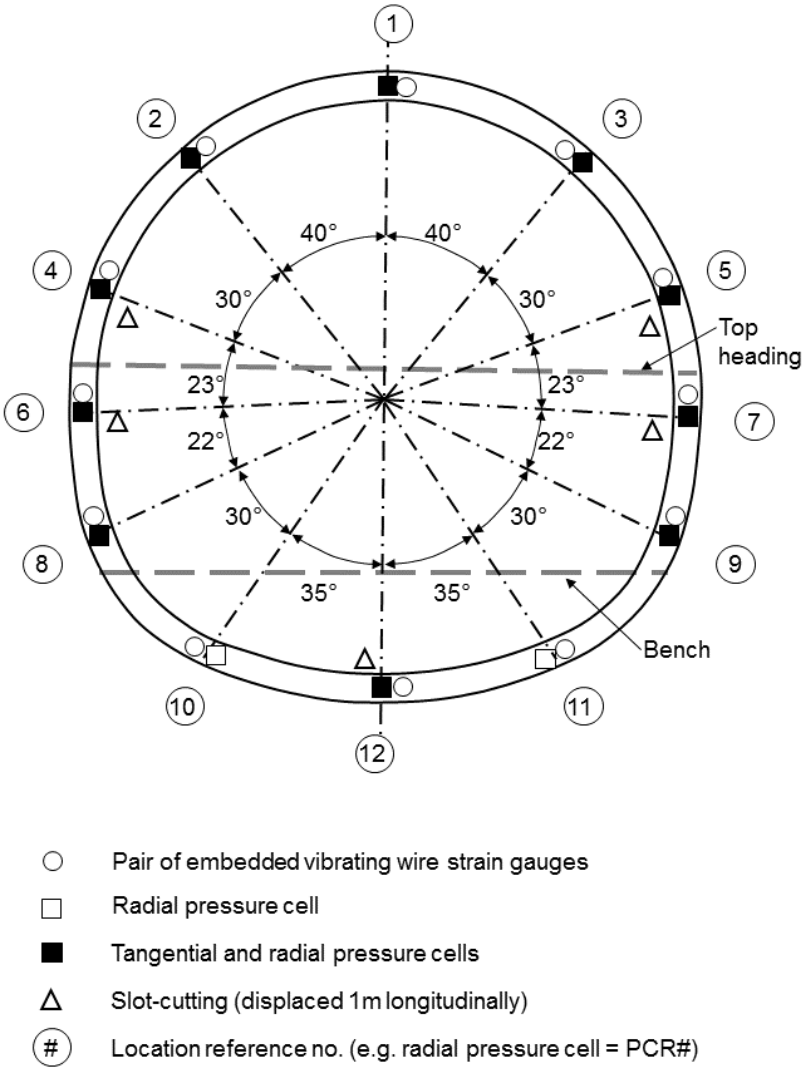

Figure 5: Main monitoring section schematically showing locations of pressure cells and strain gauges embedded in the sprayed concrete primary lining

The radial pressure cells installed in the Concourse Tunnel were Geokon model 4850-2 oil-filled vibrating wire cells, and the tangential pressure cells were Geokon model 4850-1 oil-filled vibrating wire cells. The technical specifications were given in Jones & Clayton (2021).

4 Radial stresses

A selection of the recorded radial pressures is shown in Figure 6 for MMS I and Figure 9 for MMS VIII. The positions of the radial pressure cells are marked by radial lines normal to the extrados of the lining. The outer perimeter represents the full overburden pressure of 335.4 kPa, i.e. the vertical

in situ total stress at tunnel axis level, based on a bulk unit weight for the Made Ground, Terrace Gravel and London Clay of 19.5 kN/m^3.

It is important to note that pressure cells measure total stress only, and are unable to distinguish between effective stress and pore pressure.

Where data is missing, explanations are given in the Supplementary Information.

4.1 MMS I radial stresses

At the time the secondary lining was cast approximately 1 month after installation, 10 out of 12 of the MMS I radial pressure cells were functioning well. This reduced to 7 out of 12 at 18.6 years.

The first diagram in Figure 6 shows that radial pressures built up with time around the top heading uniformly as the sprayed concrete became stiffer and the next stages were excavated and lined (c.f. Figure 3). At 15/10/96 10:00, 23 hours after spraying the top heading, the average radial pressure was 29% of the full overburden pressure.

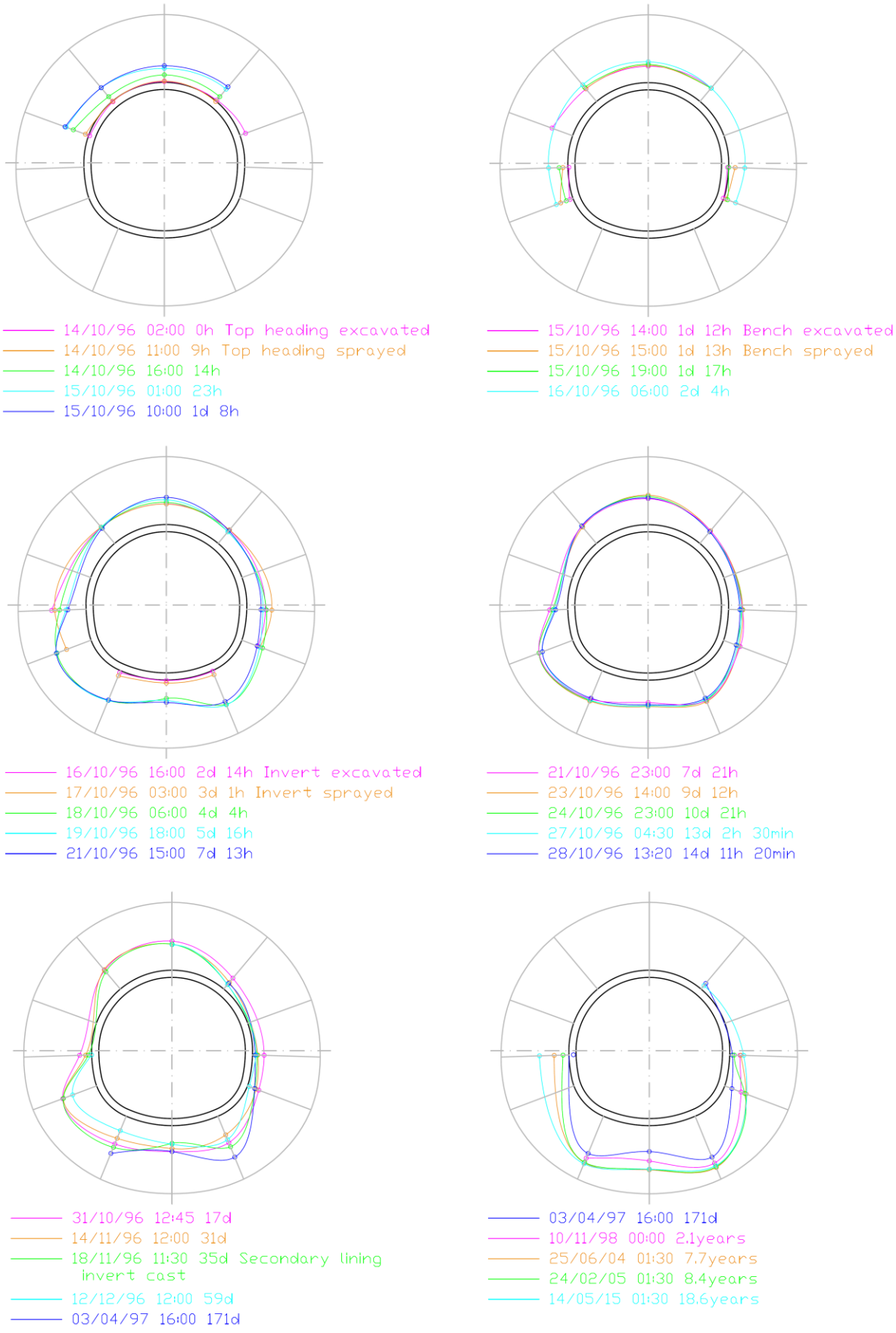

Figure 6: MMS I radial stresses (L-R, top-bottom: top heading, bench, invert, 7-14 days, 17-171 days, 171 days to 18.6 years)

When the bench was excavated and sprayed, it had little effect on the top heading pressures. Initially the bench radial pressures were small but by 16/10/96 06:00, 15 hours after spraying, the average pressures in the bench reached 81.5 kPa, 24% of the full overburden pressure.

When the invert was excavated, there was a noticeable increase in the bench radial pressures as ground arching imposed more load on the cantilevering bench sprayed concrete, which at this stage was 25 hours old and would be relatively stiff. By 18/10/96 06:00 the invert sprayed concrete was 27 hours old and radial pressures had reached a similar order of magnitude as in the bench and top heading; the sprayed concrete lining could now be said to be acting as a ring. The overall average radial pressure was 123.5 kPa, 37% of the full overburden pressure. The average radial pressure at the Crown (PCR1-5) was 29%, at the Bench (PCR6-9) 39% and at the Invert (PCR10-12) 43%.

Over the following 10 days, from 18/10/96 to 28/10/96, as the tunnel continued to advance beyond MMS I, there was very little change in the radial pressures. This was unexpected as one would expect a gradual change from front-to-back arching in the ground to circumferential arching, resulting in an increase in load on the lining.

From 31/10/96 (17 days after top heading excavation and 14 days after invert closure) to 3/4/97 (155 days later), there were some readjustments of the stress state due to casting of the secondary lining invert section, which increased the radial pressure at the invert due to the weight of concrete, and also due to temperature changes. The underpassing of the Downline Ventilation Tunnel on 3/12/96 did not have a dramatic effect but did cause a decrease in radial pressures around the invert (c.f. Figure 6).

Figure 7 shows the trend of average radial pressures and average temperatures at Crown (PCR1-5), Bench (PCR6-9) and Invert (PCR10-12) measured by thermistors attached to the radial pressure cells during this period, as a percentage of full overburden pressure. There is some correlation between temperature and radial pressures. Temperatures decreased from above 30°C during construction to below 15°C about 2 months later, resulting in a reduction in the average radial pressure. The

hydration heat from the casting of the secondary lining invert can be observed in the thermistors attached to the radial pressure cells in the invert and lasts up to 20 days. The effect of casting the rest of the secondary lining was not evident in the temperature readings in the Top Heading and Bench.

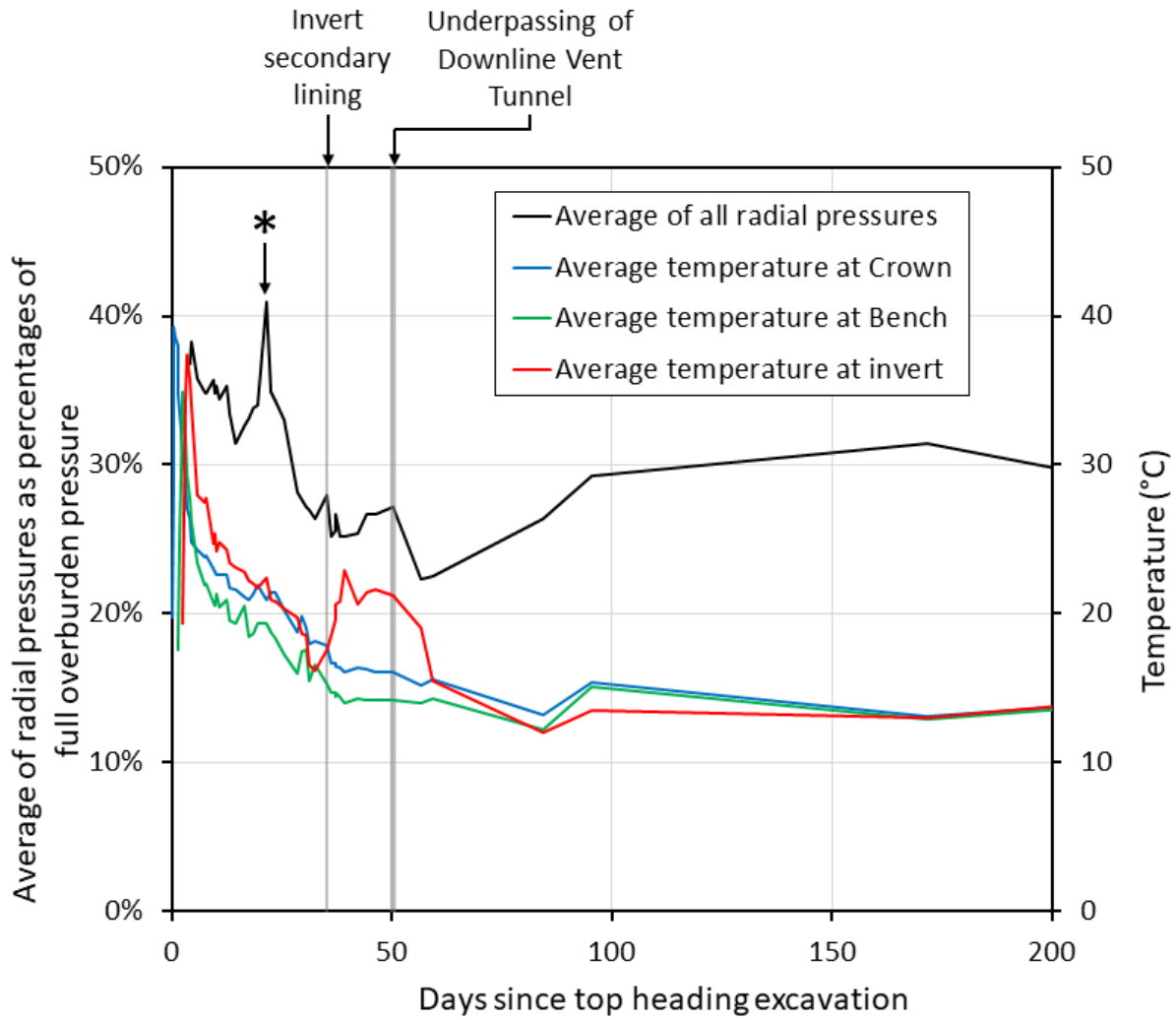

Figure 7: MMS I - average of radial pressures as percentages of full overburden pressure, and average temperatures at Crown, Bench and Invert, from invert closure to 200 days.

The relationship between the temperature of the tunnel lining and the radial pressure is due to expansion and contraction of the concrete. As temperature increases, the tunnel lining expands but is constrained by the surrounding ground, resulting in an increased radial pressure. As temperature decreases, the tunnel lining contracts and the radial pressure decreases. Therefore, the equilibrium state is constantly changing as temperature changes. This will be referred to as 'ground reaction

temperature sensitivity' (see Jones & Clayton, 2021). It represents a real stress, so will not be removed from the data.

A feature evident in Figure 7 is a rise and fall in average pressures peaking at 21 days (marked with an asterisk in Figure 7). This was experienced by all the functioning radial pressure cells to varying degrees. This was not temperature-related, and construction records do not indicate an obvious cause.

The long-term readings from 171 days to 18.6 years in Figure 6 show a slight increase in radial pressure at the invert and bench areas. The crown radial pressure cells (PCR1-5) were not reading, although there was a recovery of PCR3 at 18.5 and 18.6 years after it didn't respond at 7.7 and 8.4 years and this is shown as the average value in Figure 8 for the crown area. Therefore, it is not possible to come to any firm conclusions about radial pressures around the crown. Figure 6 shows that the tendency for PCR12 in the centre of the invert to measure a lower pressure than PCR10 and PCR11 seems to even out in the long-term. This is due to the shape of the invert: at position 12 the lower curvature makes the structural response more flexible relative to the high curvature at positions 10 and 11. This means that there is more unloading of the London Clay, and hence lower radial pressure in the short-term at position 12, whereas the stiffer structural response at positions 10 and 11 will tend to attract more radial pressure in the short-term. In the long-term, dissipation of negative excess pore pressures and the associated swelling of the clay at position 12 in the centre of the invert will tend to even out the radial pressure distribution.

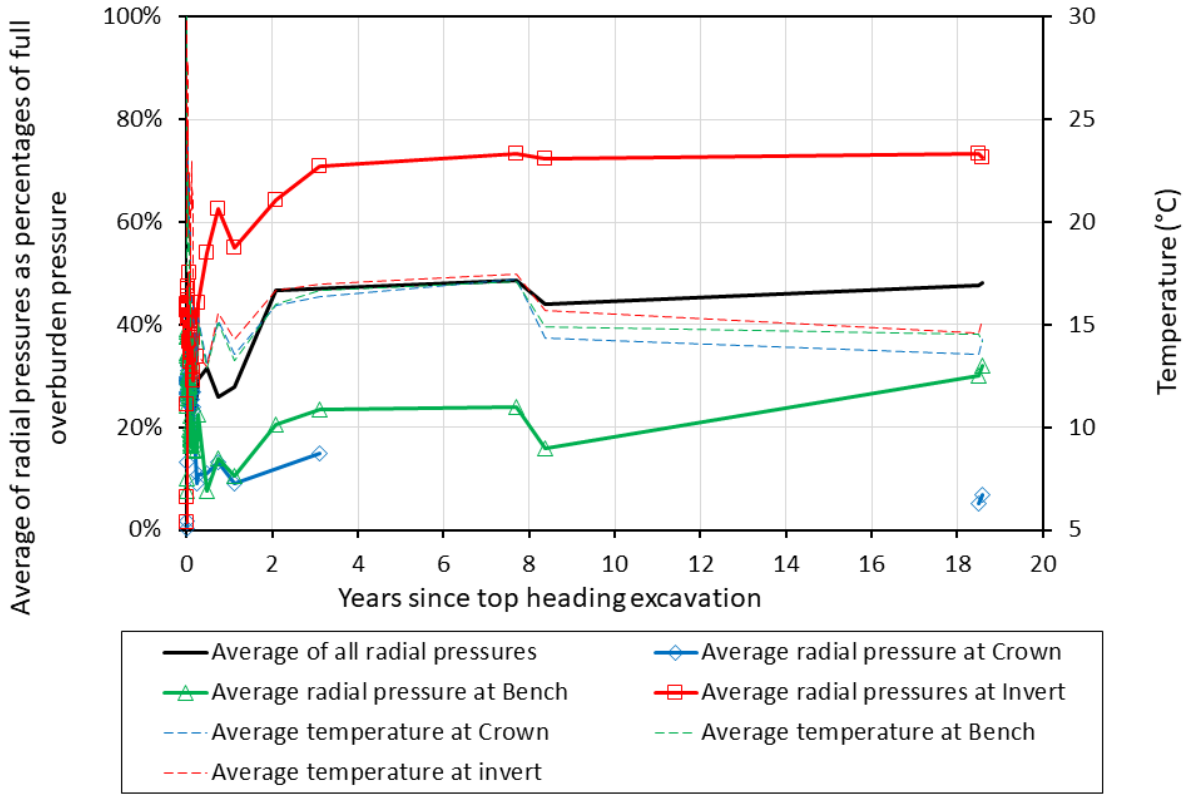

Figure 8: MMS I - average of radial pressures as percentages of full overburden pressure, and average temperatures, at Crown, Bench and Invert, from construction to 18.6 years.

4.2 MMS VIII radial stresses

Survivability of the MMS VIII radial pressure cells was much better than for MMS I. Although there were short periods when readings were not obtained from one or more radial pressure cells, all 12 were still measuring radial stresses at 8.3 years and all except PCR7 were giving readings at 18.6 years.

The first diagram in Figure 9 shows the initial readings of the top heading radial pressure cells. At the time of spraying the bench, 13.5 hours after the top heading was sprayed, the average radial pressure on the top heading was 21% of the full overburden pressure.

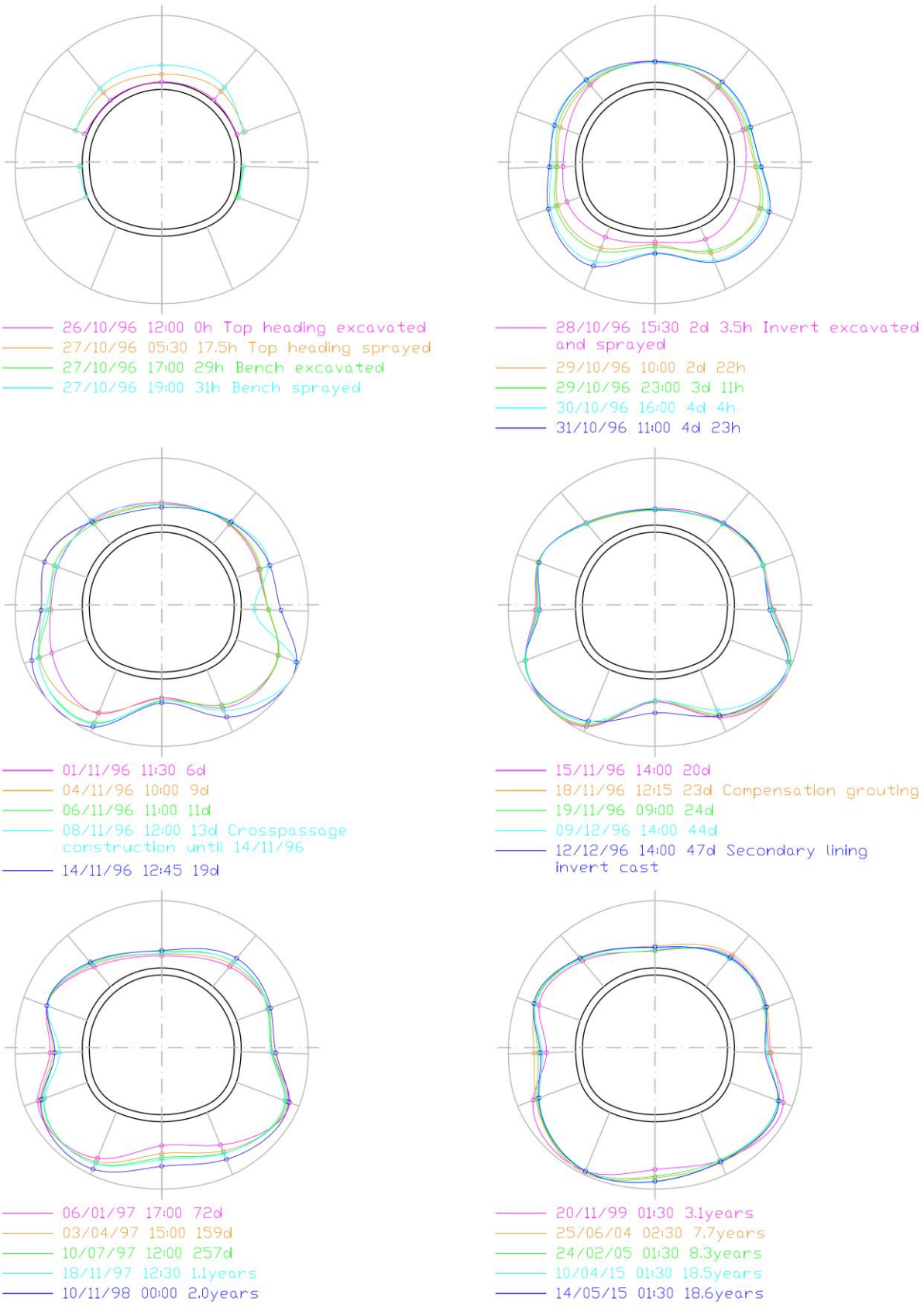

Figure 9: MMS VIII radial stresses (L-R, top-bottom: top heading & bench, invert, 6-19 days, 20-47 days, 72 days to 2 years, 3.1 years to 18.6 years).

The second diagram in Figure 9 shows that upon invert excavation the top heading radial pressures increased from 21% to 28% of full overburden pressure and the bench radial pressures had climbed to 20%. As the invert sprayed concrete became stiffer and gained strength, the lining began to act as a complete ring and pressure built up gradually at all positions except PCR1. A distinctive radial pressure distribution began to develop at the invert, with higher pressures measured at PCR10 and 11 compared to PCR12. This was also evident in Figure 6 for the MMS I radial pressure cells and the cause is attributed to the non-circular shape of the tunnel lining. At 31/10/96 11:00, almost 5 days after top heading excavation and nearly 3 days after invert closure, the average radial pressure was 43%.

The next diagram in Figure 9 shows very little change over the following week, except at PCR8 and 10 at 06/11/96 11:00, where there was a noticeable increase in pressure. Although the dates given for cross passage construction from the construction records were 07/11/96 to 14/11/96, it may be that some breaking out of the Concourse Tunnel lining occurred on 06/11/96, which would explain the change in pressure. The cross passage (c.f. Figure 1 and Figure 4) construction caused a noticeable increase in the radial pressures at the sides of the tunnel but had much less effect near the crown and invert of the tunnel, as would be expected. By 14/11/96 12:45 the radial pressure changes had stabilised, with the overall effect of the cross passage construction being an increase in average horizontal ground pressure from 51% of full overburden pressure at 04/11/96 10:00 to 62% at 14/11/96 12:45.

The 4th diagram in Figure 9 shows that from 20 to 47 days, ground pressures had stabilised with only small changes evident. Compensation grouting on the 18/11/96 did not have any effect on the radial pressures. Casting the secondary lining invert on the 12/12/96 had an effect on the radial pressures at the invert, with a significant increase at PCR12. Figure 10, which shows average pressures and temperatures at the Crown, Bench and Invert over the first 100 days, shows a significant increase in average radial pressure at the invert from 54% to 69% of full overburden pressure. This was partly

due to the additional weight and partly due to the 6°C temperature rise caused by the concrete hydration.

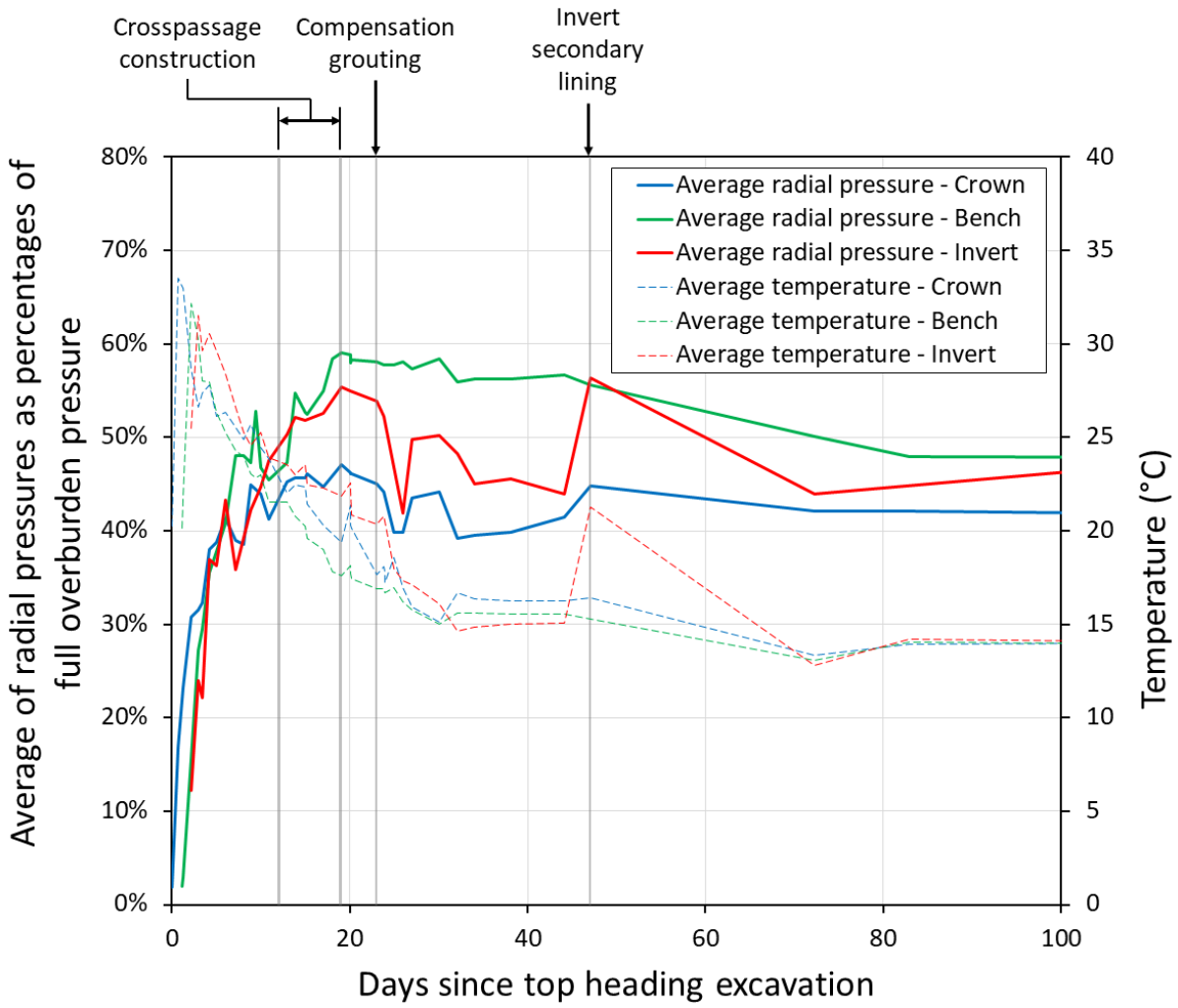

Figure 10: MMS VIII – average of radial pressures as percentages of full overburden pressure at Crown (PCR1-5), Bench (PCR6-9) and Invert (PCR10-12), and corresponding average temperatures.

From 72 days to 18.6 years (last two diagrams in Figure 9), there were only gradual changes in radial pressure, tending to increase and even out the pressure distribution. The higher level of unloading of the ground in the area around PCR12 evident soon after closure of the invert resulted in negative excess pore pressures, which over time dissipated due to groundwater flow, leading to gradually increasing radial pressure due to swelling of the London Clay.

Figure 11 shows the long-term trends of average radial pressures at the Crown, Bench and Invert. Although there was a gradually slowing increase of radial pressures, radial pressures over this

timescale were dominated by temperature effects, with a magnitude of around 7 kPa/°C. There will be no final equilibrium value of radial pressure, as it will constantly be changing as temperature changes. However, the measured radial pressures at 18.6 years were between 31% and 94% of full overburden pressure, with an average of 67%, at an average temperature of 14.2°C.

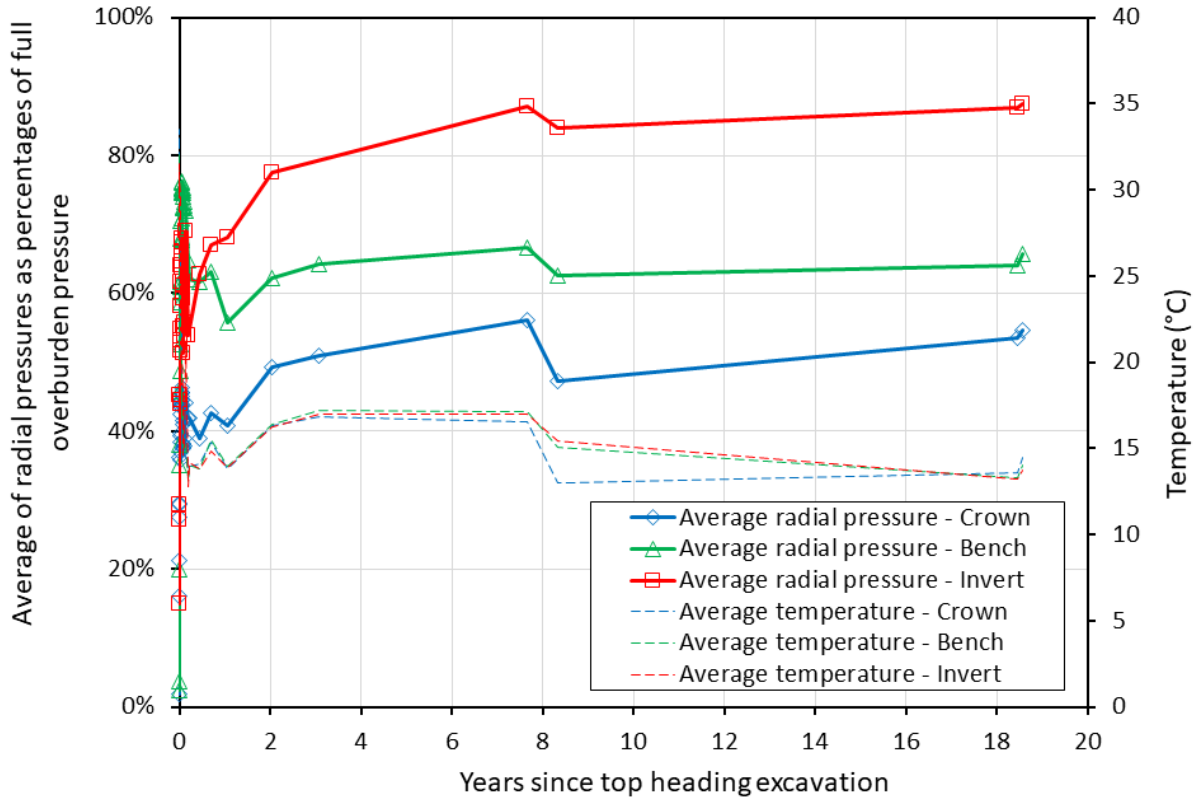

Figure 11: MMS VIII - average of radial pressures as percentages of full overburden pressure, and average temperatures, at Crown, Bench and Invert, from construction to 18.6 years.

5 Tangential stresses

The tangential pressure cell readings were interpreted according to the procedure set out in Jones & Clayton (2021), with additional details given in the Supplementary Information.

5.1 MMS I tangential stresses

Tangential stresses after adjustment for temperature sensitivity of the vibrating wire transducer, cell restraint temperature sensitivity, strain sensitivity due to shrinkage, and crimping pressures, are shown in Figure 12. The results are presented on three timescales in the three columns, from left to

right: the first 2 weeks, the first 100 days, and the full 20 years. The first two rows of charts show temperatures and tangential stresses measured by PCT1, 2 and 3 in the top heading. The next two rows of charts show temperatures and tangential stresses measured by PCT4-OUT, 4-IN, 5-OUT and 5-IN in the lower part of the top heading. The bottom two rows of charts show temperatures and tangential stresses measured by PCT6, 7, 8 and 9 in the bench and PCT12 in the centre of the invert. Remember there are no tangential cells at positions 10 and 11.

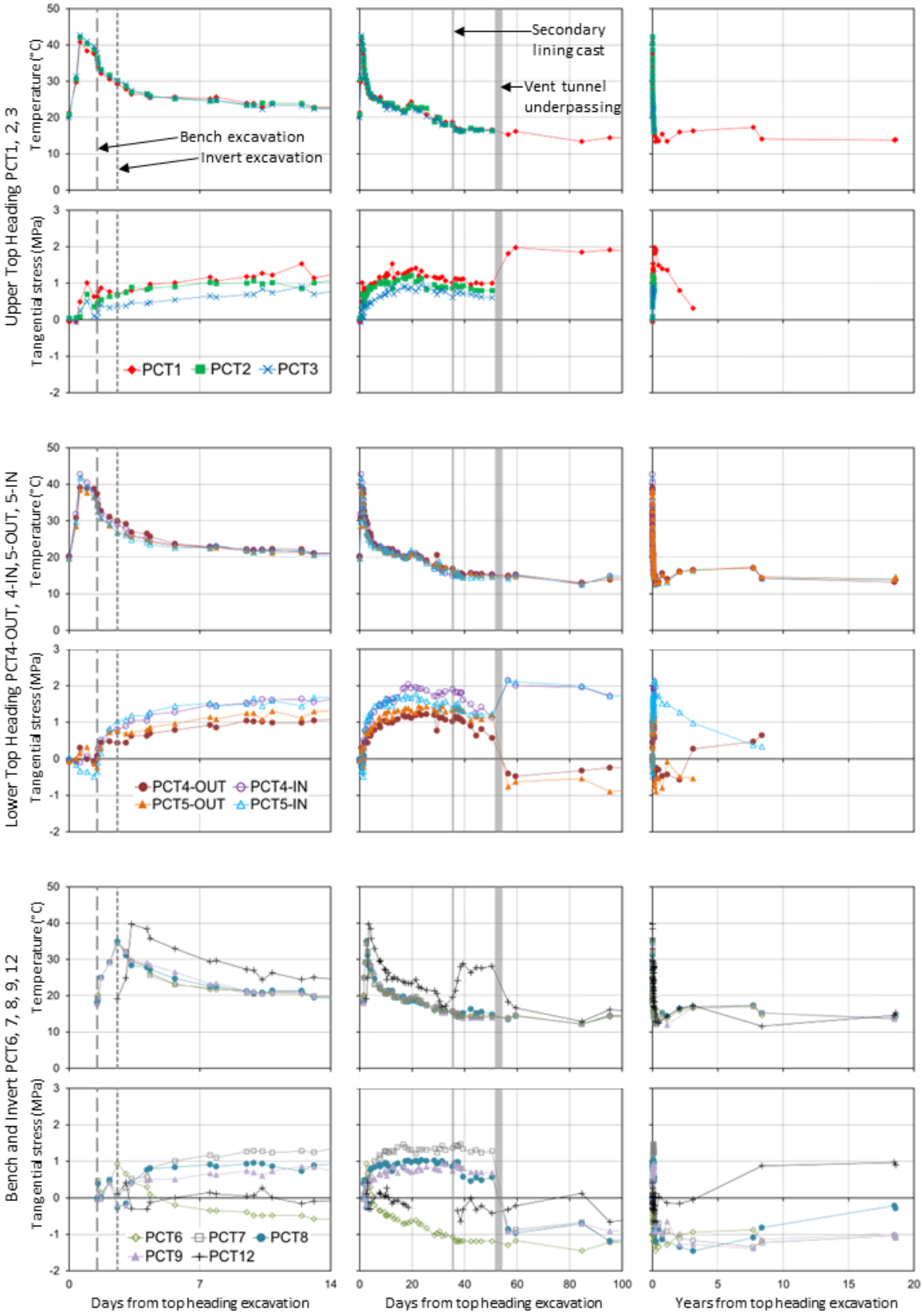

Figure 12: MMS I tangential stresses and temperatures (compression positive). Charts in the first column show the first 14 days, charts in the second column show the first 100 days, and charts in the third column show the full 20 year history.

The first column of charts in Figure 12 shows the first 2 weeks after excavation of the top heading. The delay between installation of pressure cells in the top heading and the bench at the MMS I array was approximately 36 hours, because the bench and invert were staggered behind (c.f. Figure 3). Therefore, two 1 m bench advances, one 2 m invert advance, and two 1 m top heading advances would have been excavated and lined before bench excavation at MMS I began. Tangential stress in the top heading lining reached a peak between 14 and 23 hours, before decreasing slightly. The increase and then decrease may have been caused by thermal expansion due to heat of hydration, shown in the first temperature plot in Figure 12, which was partially restrained by the ground and therefore induced a tangential stress. However, if that were the cause then one would expect to also see an increase then decrease in the radial stresses in Figure 6, but they can be seen to be monotonically increasing up to and during bench excavation. Alternatively, the rise in tangential stresses may be due to ground loading, resisted by friction between the ground and the lining, and the slight reduction in tangential stress may have been caused by undermining of the top heading during bench excavation, causing downward ground movements around the top heading, negating the interface friction and therefore reducing the tangential stress.

In the lower part of the top heading (PCT4-OUT, PCT4-IN, PCT5-OUT and PCT5-IN in Figure 12), there is a clear difference between the outer tangential cells PCT4-OUT and PCT5-OUT, and the inner tangential cells PCT4-IN and PCT5-IN. Initially the compressive stresses in the outer part of the lining were higher than in the inner part, indicating the lining may have been bending inwards (sagging), but after the full ring had been constructed this changed to a stable situation where the outer stresses were lower than the inner stresses, indicating the lining was bending outwards (hogging).

The tangential stresses in the bench (PCT6, PCT7, PCT8 and PCT9) show a smaller peak, possibly induced by hydration heat, followed by a gradual increase. The exception is PCT6, which decreased to just below zero stress.

The sole invert tangential cell PCT12 shows an increase in the first reading following installation, but this remains constant over the first 10 days and then decreases to a value between 0 and 0.25 MPa until around 20 days, when the recorded pressures become zero or negative and it must be assumed that the pressure cell has lost contact until crimping restored contact at 37 days, hence the gap in readings shown in Figure 12. Unfortunately crimping occurred at the same time as an important increase in temperature due to casting of the secondary lining invert concrete. The increase in stress due to cell restraint temperature sensitivity has been estimated and the crimping offset corrected by this amount.

Between readings at 50 and 56 days the Concourse Tunnel was underpassed by a perpendicular ventilation tunnel, as shown in Figure 1 and Figure 4. This had a dramatic effect on the tangential stresses at MMS I (Figure 12), but there was relatively little change in radial stresses (Figure 6). Usually, we would expect a tunnel to 'inverse squat' (i.e. for the vertical dimension to increase and the horizontal dimension to decrease when underpassed, but the inner tangential cells PCT4-IN and PCT5-IN showed a marked increase in stress and the outer tangential cells PCT4-OUT and PCT5-OUT showed a marked decrease in stress, indicating a hogging bending moment at these locations, which is evidence of a squatting deformation. This may be because this is not a 'greenfield' situation – the Concourse Tunnel was constructed between two already-constructed platform tunnels – so horizontal radial stresses were relatively low (Figure 6). Therefore, the temporary unloading of vertical stress due to underpassing did not cause any inward movement of the sides of the Concourse Tunnel. The longitudinal bending of the Concourse Tunnel due to the settlement trough transverse to the ventilation tunnel may have caused the hogging bending moments observed at positions 4 and 5. PCT1 showed an increase in stress during underpassing, perhaps because the vent tunnel was not directly underneath but offset by 3-4 m from MMS I, and therefore complex deformation and ground arching around the vent tunnel may have caused this increase. PCT6, PCT7, PCT8, PCT9 and PCT12 all showed a large decrease in stress. Recorded pressures in PCT4-OUT, PCT5-OUT, PCT6, PCT7, PCT8 and PCT9 all fell to near zero values at the time of underpassing. It is

therefore concluded that these tangential cells lost contact at this time, so the calculated stresses in Figure 12 should be interpreted as an upper bound and the actual stresses may have been more tensile.

In the long term, from 3 months to 18.6 years, there is no discernible increase in tangential stress, except at PCT12. In fact, many of the tangential cells show a decrease in stress compared to the values at 3 months.

5.2 MMS VIII tangential stresses

Tangential stresses after adjustment for temperature sensitivity of the vibrating wire transducer, cell restraint temperature sensitivity, strain sensitivity due to shrinkage, and crimping pressures, are shown in Figure 13. The results are presented in the same way as for MMS I, except that the first column shows the first 21 days rather than the first 14 days, so that the effect of nearby cross passage construction may be seen. Also, the pressure cells are grouped differently because there are two pressure cells at positions 6 and 7, instead of at positions 4 and 5.

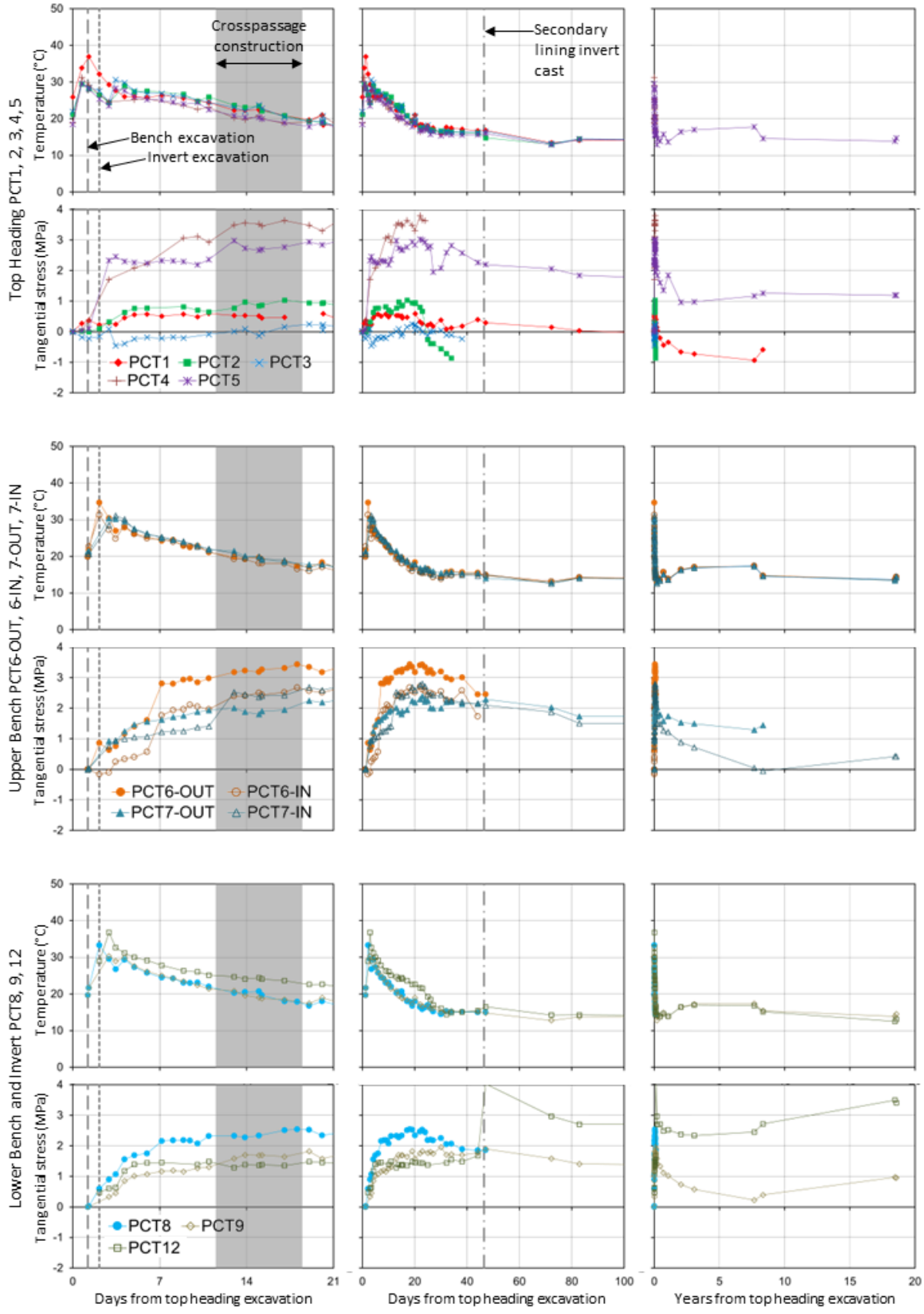

Figure 13: MMSVIII tangential stresses and temperatures. Charts in first column show the first 21 days, charts in the second column show the first 100 days, and charts in the third column show the full 20 year history.

The first column of charts in Figure 13 show the first 3 weeks after top heading excavation. Due to the staggered construction sequence, the delay from top heading to bench excavation was 29 hours, and the invert was excavated 23 hours later. Tangential stresses rose quickly at PCT4 and PCT5 to between 2 and 3 MPa at 4 days, while at PCT1, PCT2 and PCT3 they stayed below 1 MPa. At the upper bench positions 6 and 7, where 2 tangential cells were placed side-by-side to measure bending moments, initially higher stresses were measured by the outer cells compared to the inner cells. When cross passage construction began, PCT7-OUT measured a slight decrease in tangential stress and PCT7-IN measured an approximately 1 MPa increase, whereas at position 6 no significant changes were evident. This is consistent with what happened to the radial pressures in MMS VIII, with PCR7 registering larger changes than PCR6 on the opposite side. The reason for this is unknown but may be related to way the cross passage opening was broken out or may be due to the timing of the breakout relative to the times that pressure cell readings were taken, which at this stage was only once per day.

The second column of charts in Figure 13 show the first 100 days after top heading excavation. Over this time period, temperatures gradually decreased from the peak of 30-40°C caused by hydration heat to approximately 14°C. Tangential stresses reached a maximum at most positions at about 5-10 days, then gradually decreased up to 100 days. Casting of the secondary lining invert at 46.5 days caused a significant increase in tangential stress measured by PCT12, as expected. However, the temperature measured by the thermistor attached to PCT12 only measured an increase of 1°C. This must have been a misreading because the thermistor attached to radial cell PCR12 measured an increase up to 26.7°C, and PCT12 should be expected to have risen higher than that, being closer to the source of hydration heat.

The third column of charts in Figure 13 show the full history of temperature and tangential stress up to 18.6 years. Only four pressure cells were both still functioning and had not lost contact, PCT5,

PCT7-IN, PCT9 and PCT12. In the long term there was a trend for the invert tangential stresses to increase with time, which is consistent with the results from the radial pressure cells.

5.3 Slot-cutting

Slot-cutting was also performed at five positions at both MMS I and MMS VIII (see Figure 5) by Cardiff University (Hughes, 1997) approximately 1 month after MMS I construction and approximately 3 weeks after MMS VIII construction. A rectangular slot 230 mm wide and 110 mm deep was created by stitch-drilling, while displacements of measuring studs 30 mm above the slot were measured using LVDT gauges attached to a rigid measuring frame. A mini flat jack 228 x 117 mm in plan was then inserted and then the pressure was increased in the jack to reverse the displacements.

The results showed tensile or near-zero stresses at all the five positions on both the cross-sections. During cutting, the studs actually moved away from the slot, indicating that the concrete had been in tension. Drying shrinkage of the intrados of the lining put the concrete in tension and the reinforcement into compression, so that when the slot was cut, the reinforcement pushed it open. When the reinforcement was then cut, the slots would close again, although not enough to return to zero stress in most cases.

6 Discussion and conclusions

A valuable case study has been presented, which when added to previously published monitoring of surface and subsurface ground movements of the same tunnel by van der Berg et al. (2003) and Clayton et al. (2006), will reduce uncertainty in design, and help designers and researchers to calibrate numerical models.

Survivability of the pressure cells was an issue and it was fortunate that so many were installed in each section. 10 out of 24 tangential cells were still functioning at 18.6 years. However, of these 10, four had descended to zero and later readings had to be ignored. This could have been prevented by crimping. The radial pressure cells fared much better, with 18 out of 24 still functioning at 18.6 years. The reasons why instruments stopped working is unknown, but some at least may be due to cable damage. It is recommended that future installations plan for redundancy with multiple arrays and more pressure cells in each array than strictly required.

A handheld vibrating wire reader was used and to take a set of readings of all the pressure cells and strain gauges in one array took 1-2 hours. This meant that readings were only taken once or twice per day for the first 2 weeks, then once per day up to around 6 weeks. This frequency was suboptimal during the first week when changes in stress state were occurring rapidly as the tunnel continued to be excavated and lined ahead of the array. Similarly, a higher frequency of readings during underpassing of the vent tunnel at MMS I and during cross passage construction at MMS VIII would have allowed more detailed analysis of the response. At least one reading per hour during these periods would be the minimum desirable, but higher frequencies can easily be achieved by using automatic data logging and so a frequency of every 10 minutes is recommended. For the rest of the construction period, one reading per hour is recommended and for the long term, once per week is recommended with one day per month having readings every hour to capture any diurnal temperature variation effects.

The effect of underpassing of MMS I, cross passage construction close to MMS VIII, and the casting of the secondary lining invert section at both monitoring sections was observed in the pressure cell measurements. Underpassing caused a small but measurable reduction of radial pressure around the bench and invert of MMS I, but the effect on the tangential stresses was rather more dramatic with large bending moments induced in the lining.

Cross passage construction close to MMS VIII caused a noticeable increase in the radial pressures at the sides of the tunnel but had much less effect near the crown and invert of the tunnel, as would be expected. This increase was caused by ground arching around the breakout. The effect was more noticeable on the right-hand side of the tunnel looking inbye (the western side in Figure 1). Tangential stresses were also affected, with a noticeable bending moment induced at position 7, also on the right-hand side of the tunnel. The reason for the larger effect on one side of the tunnel rather than the other may have been due to the timing of pressure cell readings and how they coincided with construction stages of the cross passages.

Casting of the secondary lining invert section caused an increase in radial pressure at the invert due to thermal expansion and added weight. There was also an increase in tangential stress in the invert.

Slot-cutting stress measurements in the inner 120 mm of the 350 mm thick primary lining made approximately 1 month after construction indicated zero or tensile stress at all five points measured, at both MMS I and MMS VIII. The main cause of this tension was probably drying shrinkage.

Variation of stress and strain through the thickness of the primary lining due to axial forces, bending moments and shrinkage means that tangential pressure cells centred in the middle of the lining will always provide more variable results than radial pressures. In general, pressure cells are very sensitive to small changes in stress and provide useful information. A more detailed interpretation would have been possible for this case study if the pressure cells had been read more frequently using an automatic datalogger, and if tests had been undertaken on the shotcrete to determine the parameters needed for the interpretation of the tangential pressure cells, especially the final shrinkage $\varepsilon_{sh,\infty}$ and shrinkage parameter B.

Radial pressures stabilised after construction activities had ceased at a value that was at most locations well below full overburden pressure. These did not increase in the long-term, except around the invert where at one point radial pressure reached 94% of full overburden pressure. This may be due to the greater degree of unloading and the negative excess pore pressures generated in

the London Clay around the invert during construction that then dissipated over time causing swelling of the clay. The degree of unloading and the effect on pore pressures around the tunnel may explain the differences in rate and maximum value of ground load development noted in previous case studies.

Values of maximum load as a percentage of hydrostatic full overburden pressure are shown in Table 1, along with the range of values found at MMS VIII after 18.6 years. With the exception of Skempton (1943) and Ward & Thomas (1965), the results from this case study are broadly in line with other case studies in London Clay. Differences may be caused by the degree of unloading of the ground during construction, whether the tunnel acts as a drain on the ground around it, and whether there is temperature change in the long-term.

Authors	**Tunnel**	**Maximum load (% hydrostatic overburden)**
Bowers & Redgers 1996	Jubilee Line Extension, St. James's Park	43-62 %
Barratt *et al*. 1994	Jubilee Line, Regent's Park	40-64 %
Muir Wood 1969	Heathrow Cargo Tunnel, Heathrow	60-80 %
Ward & Thomas 1965	'Site V', Victoria Line	105 %
Ward & Thomas 1965	'Site O', London	71 % (not stabilised)
Cooling & Ward 1953	9' diameter water tunnel, London	53-64 %
Skempton 1943	Unknown, London.	102-108 %
This study (MMS VIII)	*Heathrow T4 Concourse Tunnel*	*40-94 %*

Table 1: Maximum stresses measured in tunnel linings in London Clay expressed as a percentage of hydrostatic full overburden pressure

Tunnels do not have a single long-term state of equilibrium. As temperature in the tunnel increases and decreases, the tunnel lining expands and contracts against the ground, increasing and decreasing the radial pressure at the ground-lining interface. This has been termed 'ground reaction temperature sensitivity'. In some cases, for instance for London Underground tunnels where during tunnel operation the temperature in the lining and the surrounding ground has gradually increased over many years (Stephen, 2016), one may expect a gradual long-term increase in lining stress as a result.

Pressure cells measure total stresses, and so they cannot tell us whether the groundwater pressure was applied to the primary or secondary lining in the long-term. After casting of the secondary lining,

the crown was grouted between the waterproof membrane and secondary lining to fill any voids. Nevertheless, there would need to be a significant increment of ground load for the primary lining to deform sufficiently to begin to share load with the secondary lining. Unfortunately, no instruments were installed in the secondary lining and this should be considered for future projects.

7 References

Barratt, D. A., O'Reilly, M. P. & Temporal, J. (1994). Long-term measurements of loads on tunnel linings in overconsolidated clay. *Proc. Tunnelling '94*, pp.469-481. London: IMM.

Bowers, K. H. & Redgers, J. D. (1996). Discussion: Observations of lining load in a London Clay tunnel. *Proc. Int. Symp. on Geotechnical Aspects of Underground Construction in Soft Ground* (eds. Mair & Taylor), London, UK. Rotterdam: Balkema.

Byfors, J. (1980). *Plain concrete at early ages,* CBI Forskning Fo 3:80, 464pp. Stockholm: Swedish Cement and Concrete Research Institute.

Chang, Y. & Stille, H. (1993). Influence of early age properties of shotcrete on tunnel construction sequences. *Proc. Shotcrete for Underground Support VI* (eds. D. F. Wood and D. R. Morgan), Niagara-on-the-lake, Canada, pp.110-117. USA: ASCE.

Clayton, C. R. I., van der Berg, J. P., Heymann, G., Bica, A. V. D. & Hope, V. S. (2002). The performance of pressure cells for sprayed concrete tunnel linings. *Géotechique* **52**, No.2, 107-115.

Clayton, C. R. I., van der Berg, J. P. & Thomas, A. H. (2006). Monitoring and displacements at Heathrow Express Terminal 4 station tunnels. *Géotechnique* **56**, No.5, 323-334.

Cooling, L. F. & Ward, W. H. (1953). Measurements of loads and strains in earth supporting structures. Proc. 3rd ICSMFE, Session 7/3, Vol.2, pp.162-166.

Hight, D. W., Gasparre, A., Nishimura, S., Minh, N. A., Jardine, R. J. & Coop, M. R. (2007). Characteristics of the London Clay from the Terminal 5 site at Heathrow Airport. *Géotechnique* **57**, No.1, 3–18.

Hughes, T. G. (1997). *Flat jack investigation of Heathrow Terminal 4 concourse tunnel 13-19th November 1996*. Report by Cardiff School of Engineering, University of Wales for the University of Surrey.

HSE (1996). *Safety of New Austrian Tunnelling Method (NATM) tunnels*, Health and Safety Executive, 86pp. London: HSE Books, HMSO.

Jones, B. D. (2005). *Ageing shells*. Internal report, Mott MacDonald.

Jones, B. D. & Clayton, C. R. I. (2021). Interpretation of tangential and radial pressure cells in and on sprayed concrete tunnel linings. *Underground Space* **6**, No.5, 516-527.

King, C. (1981). The stratigraphy of the London Basin and associated deposits. *Tertiary Research Special Paper* **6**. Rotterdam: Backhuys.

Kuwajima, F. M. (1999). Early age properties of the shotcrete. *Proc. Shotcrete for Underground Support VIII* (eds. T. B. Celestino and H. W. Parker), São Paulo, Brazil. Reston, Virginia, USA: ASCE.

Muir Wood, A. M. (1969). Written contribution, plenary session 4. *Proc. 7th Int. Conf. Soil Mechanics and Foundation Engineering*, Vol.3, Mexico, pp.363-365.

Powell, D. B., Sigl, O. & Beveridge, J. P. (1997). Heathrow Express – design and performance of platform tunnels at Terminal 4. Proc. Tunnelling ’97, London, pp.565-593. London: IMM.

Skempton, A. W. (1943). Discussion: Tunnel linings with special reference to a new form of reinforced concrete lining, by G. L. Groves. *J. Instn Civ. Engrs* **20**, No.5, March, 53-56.

Stephen, P. (2016). Cooling the Tube. *Rail Magazine*, 3rd February 2016, https://www.railmagazine.com/infrastructure/stations/cooling-the-tube [last accessed 28th March 2023].

van der Berg, J. P., Clayton, C. R. I., Powell, D. B. & Savill, M. (1998a). Monitoring of the Concourse Tunnel at Heathrow Express Terminal 4 station constructed using the NATM. *Tunnels and Metropolises*, Proc. World Tunnel Congress (eds. A. Negro Jr. and A. A. Ferreira), São Paulo, Brazil, pp.1163-1168. Rotterdam: Balkema.

van der Berg, J. P., Clayton, C. R. I. & Hope, V. S. (1998b). An evaluation of the role of monitoring during the construction of shallow NATM tunnels in urban areas. *Proc. North American Tunnelling '98* (ed. L. Ozdemir), Newport Beach, California, USA, pp.251-257.

van der Berg, J. P., Clayton, C. R. I. & Powell, D. B. (2003). Displacements ahead of an advancing NATM tunnel in the London clay. *Géotechnique* **53**, No.9, 767-784.

Ward, W. H. & Thomas, H. S. H. (1965). The development of earth loading and deformation in tunnel linings in London Clay. Proc. 6th ICSMFE, Vol.2, Divisions 3-6, Montreal, Canada, 8th-15th September, pp.432-436.